JOURNAL OF Applied Polymer SCIENCE

Special Issue: Sustainable Polymers and Polymer Science Dedicated to the Life and Work of Richard P. Wool

Guest Editors: Dr Joseph F. Stanzione III (Rowan University, U.S.A.)
and Dr John J. La Scala (U.S. Army Research Laboratory, U.S.A.)

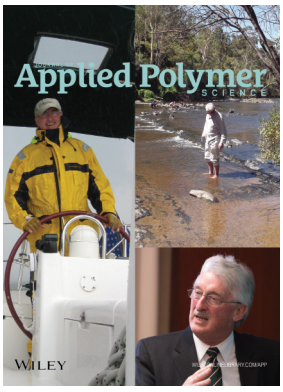

EDITORIAL

REVIEWS

RESEARCH ARTICLES

JOURNAL OF Applied Polymer SCIENCE

Special Issue: Sustainable Polymers and Polymer Science Dedicated to the Life and Work of Richard P. Wool

Guest Editors: Dr Joseph F. Stanzione III (Rowan University, U.S.A.)
and Dr John J. La Scala (U.S. Army Research Laboratory, U.S.A.)

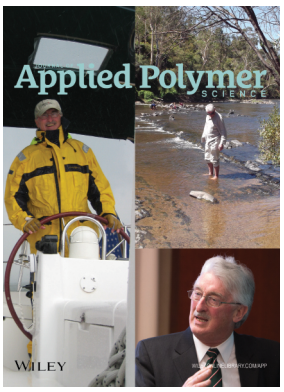

Journal of Applied Polymer Science

Semi-IPN of biopolyurethane, benzyl starch, and cellulose nanofibers: Structure, thermal and mechanical properties

Md Minhaz-Ul Haque,[1] Kristiina Oksman[1,2]
[1]Division of Materials Science, Luleå University of Technology, Luleå SE 97187, Sweden
[2]Fiber and Particle Engineering, University of Oulu, Oulu FI 90014, Finland
Correspondence to: K. Oksman (E-mail: kristiina.oksman@ltu.se)

ABSTRACT: The aim of this study was to develop bionanocomposites of biopolyurethane (PU), benzyl starch (BS), and cellulose nanofibers (CNF) with semi-interpenetrating polymer network (S-IPN) structure of improved properties. Morphology, thermal and mechanical properties of S-IPN blends and nanocomposites were studied and compared with the neat polymers. Microscopy study showed that PU and BS were partially miscible as well as CNF were dispersed in both PU and BS phases in the nanocomposites. Dynamic mechanic thermal analysis demonstrated that BS decreased the tan δ peak of the PU while CNF increased it. The positive shifting of tan δ peak in the S-IPN nanocomposite also indicated the presence of CNF in the PU phase. It was also noticed that S-IPN nanocomposite displayed two tan δ peaks at higher temperature, indicating molecular interaction among BS, PU, and CNF. Furthermore, the S-IPN nanocomposites displayed significantly higher E-modulus and tensile strength compared with the neat PU.
 J. Appl. Polym. Sci. **2016**, *133*, 43726.

KEYWORDS: biopolymers and renewable polymers; cellulose and other wood products; composites; crosslinking; mechanical properties

Received 17 January 2016; accepted 4 April 2016
DOI: 10.1002/app.43726

INTRODUCTION

The sustainable and renewable materials are of interest today because of our limited petroleum reserves and plastic wastes results in environmental pollution. Many of these problems could be solved by using polymers and materials from renewable resources. Renewable or biobased polymeric materials, e.g. cellulose, starch, poly(lactic acid), etc. have much potential and several advantages, such as biodegradability, renewability, sustainability, etc. In spite of several advantages of renewable polymers, their properties are still far from those of the common used petroleum-based polymers. Therefore, development of new materials through the modification of biobased polymeric materials is a great attention of industrial and academic research. One convenient modification technique is blending. In contrast to the synthesis of novel polymers from these materials, the development of new materials by blending the existing biobased materials is a comparatively economic route.[1] However, the properties of natural polymers, their blends, and composites are usually low depending on that they are immiscible and thermodynamically incompatible. As a result, the mixed components display macrophase separation with low adhesion towards each other and such materials will lead to poor mechanical properties.[2] Various strategies such as modification of polymers by graft-copolymers,[3–5] addition of compatibilizers[1,26] or creating of interpenetrating polymer networks (IPN),[7–10] etc. can be used to minimize the polymer phase separation.

According to IUPAC, the definitions of IPN is "Polymer comprising two or more *networks* that are at least partially interlaced on a molecular scale but not covalently bonded to each other and cannot be separated unless chemical bonds are broken". On the other hand, semi-IPN is "Polymer comprising one or more *polymer networks* and one or more linear or branched polymers characterized by the penetration on a molecular scale of at least one of the *networks* by at least some of the linear or branched macromolecules.[11] IPN is an important technology of blending of polymers, which helps in mixing incompatible polymers. Polymer blend based on IPN exhibit better dispersion of phases and stability in morphology by decrease of the interfacial tension of phases.[12] Therefore, higher mechanical properties are expected by interpenetrating polymer networks in contrast to the normal polymers blend. The IPN also find many industrial applications based on different polymers, particularly polyurethanes such as impact-resistant materials, materials for sound proofing and thermal insulation, solid electrolytes, conducting elastomers coatings, adhesives, and so on.[13] IPN can also be used in biomedical applications such as preparation of

hydrogels and their applications in controlled drug delivery.[14] In the present study, a new S-IPN nanocomposite with improved properties based on biobased polyurethane (PU), benzyl starch (BS) derived from potato starch, and cellulose nanofibers (CNF) isolated from banana rachis waste was prepared.

Polyurethanes are interesting materials owing to their wide variety of applications, such as foams, elastomers, adhesives and coatings, etc. The choice of the PU matrix can be dictated by the fact that they can be synthesized from renewable polyol, like soybean oil,[15] castor oil,[9] palm oil,[16] linseed oil,[17] etc. Moreover, synthesis of polyurethanes is relatively easier and they have been using in the synthesis of many IPNs.[18–22] PU can be used with BS[9] to form S-IPN and it is also compatible with cellulose nanoparticles.[23,24] It has been reported that S-IPN materials based on PU and BS showed improved mechanical properties compared with the neat PU.[9] More improvement in mechanical properties of the PU and BS based S-IPN materials can be expected by the presence of CNF. The reinforcing effect of nanocelluloses obtained from different sources e.g., sisal,[25] wood,[26] tunicate,[27] wheat straw,[28] banana,[29,30] etc. are also promising for many polymers because of their mechanical properties.[23,24,31–35] Hence, combination of PU, BS, and CNF based on IPN can develop a new nanocomposite material with improved properties. Moreover, publications concerning the preparation and properties of interpenetrating polymer networks based CNF nanocomposites are relatively uncommon.

Thus, the aim of the present study was to create a new S-IPN nanocomposite with improved properties based on PU, BS derived from potato starch and CNF. The S-IPN nanocomposite was planned to prepare by casting process. It was reported that CNF as hydrogen-bonded CNF network has a very large reinforcing effect in polymer nanocomposites obtained by the casting process.[36] The hypothesis of the work was that if a blend of BS and CNF are mixed with the prepolymers (polyol and isocyanate) of PU and a network of PU is thereafter created by the chemical reaction between polyol and isocyanate, then the resulting material can exhibit improved mechanical properties because of the semi-interpenetrating polymer network of PU and BS (which has been reported by Cao *et al.*[9]) as well as the reinforcement of CNF by forming hydrogen-bonded CNF network. In this study 10–30 wt % of BS content were used to prepare S-IPN nanocomposites. Generally, the natural polymer content in S-IPN materials should be <30 wt % to get improvement in mechanical properties.[9] The concentration of CNF was selected 10 wt % considering the large reinforcing effect in starch.[34] The S-IPN nanocomposite morphology, thermal and mechanical properties were studied

EXPERIMENTAL

Materials

Matrix Components. Polyol (Polygreen 3110) based on palm oil with a minimum hydroxyl value of 92 mg KOH/g, viscosity of 1200 mPas at 30 °C, functionality of 2 and acid number of 0.7 mg KOH/g was supplied by PolyGreen, Malaysia. Commercial polymeric methane di-phenyl di-isocyanate (PMDI) (ISO PMDI 92140) with –NCO content of 31%, functionality of 2.7, density of 1.23 g/cm^3 at 25 °C, melting point of <10 °C, and viscosity (dynamic) of 170–250 mPas (25 °C) was purchased from Lagotech AB, Sweden. Dibutyltin dilaurate (DBTDL) as a catalyst (laboratory-grade) were purchased from VWR, Sweden

Potato starch (water content 20 wt %, BDH, Prolabo), Benzyl chloride (purity 99.0%, Alfa Aesar. GmbH and Co, KG, Germany), and Sodium hydroxide (NaOH) pellets (purity 99.0%, Merck, Germany) were purchased from VWR, Sweden.

Solvent and Swelling Agent. N,N-dimethylformamide (DMF), purity 99.8% were purchased from Sigma-Aldrich, Sweden.

Reinforcing agent: CNF were prepared from bleached cellulose pulp obtained from banana rachis waste (received from the Pontifical Bolivarian University Colombia) using mechanical fibrillation, as reported in elsewhere.[37] Firstly, 2 wt % of the aqueous cellulose pulp suspension was prepared by a high shear mixer (L4RT, Silverson, England). CNF were then obtained by grinding the cellulose suspension at 1000 rpm by passing through a supermass colloider (Masuko MKZA10–20J, Japan).

Preparation of S-IPN Blends and Nanocomposites

Benzylation of starch or starch-CNF blend followed the procedure reported by Cao *et al.*[9] In a three-necked round bottom flask connected with a condenser, 10 g of starch previously dispersed in 100 mL of water was taken and heated at 40 °C using an oil bath. The mixture was stirred strongly using a mechanical stirrer and 35 wt % of NaOH solution (50 g) was added drop-wise through a dropping funnel. The stirring was continued for 30 min more and then 25 g of benzyl chloride was added. The temperature was increased upto 100 °C and the benzylation reaction was carried out for 1 h. A white gummy precipitate of BS was separated and washed with acetone and water several times. Finally, washed BS was dried under vacuum and stored in a desiccator. Benzylation of the starch-CNF blend of required weight ratio was carried out by following the above procedure to obtain benzylated starch-CNF (BS-CNF) blend. In this case starch powder was premixed with CNF aqueous suspension. The procedure of the synthesis of BS with a reaction scheme is shown in Figure 1.

The palm-oil-based PU film (NCO/OH = 1.2) and S-IPN films of PU/BS, PU/BS/CNF were synthesized as reported by Cao *et al.*[9] with some modifications. PMDI (2.11 g) with DMF was taken into a two-necked round bottom flask and then 7.89 g of palm-oil-based di-polyol (hydroxyl groups content 4.49 wt %) dissolved in DMF was added into the flask drop-wise for 50 min under a nitrogen atmosphere. The mixture was stirred for 2 h. The resulting PU prepolymers were mixed with BS or BS-CNF blend of a desired mass (previously dissolved or dispersed in DMF) for 5 min; finally, 1 wt % of catalyst of DBTDL was added and mixing was continued for 1 min. The resultant mixture of 5 wt % solid content (10 wt % for PU) was cast onto Teflon petri dishes. The cast material was then kept in an oven at 60 °C for 12 h to carry out curing. Thus the films of PU, PU/BS S-IPN blends, and PU/BS/CNF S-IPN nanocomposites were obtained. A nanocomposite film based on PU and CNF was also prepared following the above procedure. In this case, dispersion of CNF in DMF was obtained by exchanging water with acetone and then acetone with DMF through several steps of

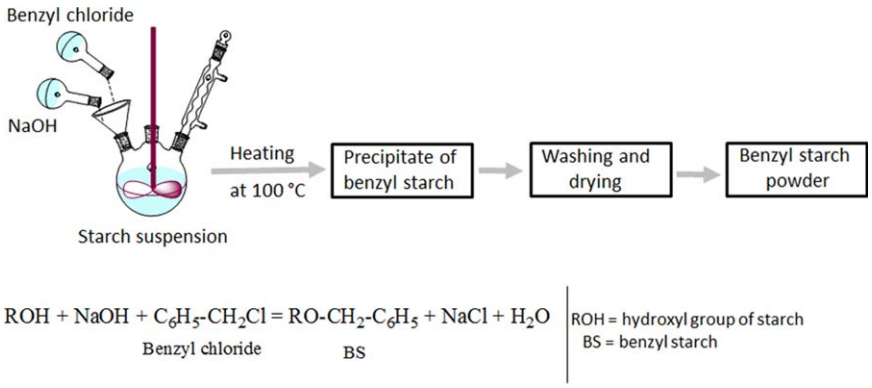

Figure 1. Follow diagram for synthesis of benzyl starch with a reaction scheme. [Color figure can be viewed in the online issue, which is available at wileyonlinelibrary.com.]

centrifugation and re-dispersion. The prepared materials were coded as reported in Table I.

Characterization

Starch and BS were analyzed by FT-IR spectroscopy to be confirmed that benzylation of starch was occurred. The samples were analyzed with KBr pellets using a Bruker IFS 66v/S FTIR spectrometer by averaging 120 scans at a resolution of 4 cm^{-1}.

The morphology of the used CNF was examined by using a Veeco multimode atomic force microscopy (AFM) (Santa Barbara, USA), with a Nanoscope V controller with etched silicon tips, operating in the taping mode in air. A droplet of CNF suspension (about 0.02 wt %) was put on fresh mica plate and dried it at 60 °C under vacuum for 1 h. The dried sample was then analyzed and height and amplitude images were collected.

Cryogenically fractured surfaces of neat PU, the S-IPN blends, and the S-IPN nanocomposite were studied using a high-resolution scanning electron microscope (HR-SEM) (Merlin Zeiss, Germany) to study the structure and the effect of CNF addition in the morphology. The sample surfaces were coated using a Bal-Tec MED 020 Coating System with a tungsten target. The coating was performed in a vacuum of approximately 6×10^{-5} mbar with 100 mA current for 20 s to obtain about 3–5 nm coating thickness.

Gel content of neat PU, S-IPN blend and nanocomposite was determined of small rectangular film specimens (approximately 0.1 g) in DMF at room temperature for one week. The films, enclosed in metal net pouch, were immersed in DMF with mild stirring. After 24 h DMF was replaced with fresh solvent and stirring was continued at room temperature for another 6 days. After 7 days the swollen samples were weighed with the aid of a weighing bottle. Finally, the samples were place in an oven and dried under vacuum at room temperature to obtain gel content. Swell ratio was calculated by the following equatio[38,39]:

$$\text{Swell ratio} = \frac{w_g - w_d}{w_o - w_e} K + 1 \quad (1)$$

where W_o is the original weight of polymer, W_e the weight of extract, W_g the weight of swollen mass after 7 days, W_d the weight of dried gel, and K the density of polymer/density of solvent at room temperature.

Dynamic mechanical thermal analysis (DMTA) of neat PU, S-IPN blends and nanocomposites was conducted by a DMA QA 800 from TA Instruments (USA). The rectangular sample specimens (about $20 \times 6 \times 0.3$ mm^3) were analyzed in tensile mode from −50 °C to 250 °C by setting heating rate and frequency 3 °C/min and 1 Hz, respectively.

Thermogravimetric analysis (TGA) was conducted in a TGA-Q500 from TA Instruments (USA) in air atmosphere. About 6–15 mg of samples were heated in ramp mode from 30 °C to 600 °C using a heating rate of 10 °C/min.

The tensile tests of neat PU, S-IPN blends, and nanocomposites were carried out by a conventional Shimadzu AG-X universal testing machine (Kyoto, Japan) with a load cell of 1 kN, gauge

Table I. Samples with their Coding and Compositions

Sample code	Type of materials	Compositions (wt %)			PU/BS wt. ratio
		PU	BS	CNF	
PU	—	100	—	—	—
PU90/BS10	S-IPN	90	10	—	90/10
PU80/BS20	S-IPN	80	20	—	80/20
PU72/BS18/CNF10	S-IPN	72	18	10	80/20
PU70/BS30	S-IPN	70	30	—	70/30
PU63/BS27/CNF10	S-IPN	63	27	10	70/30
PU95/CNF5	—	95	—	5	—

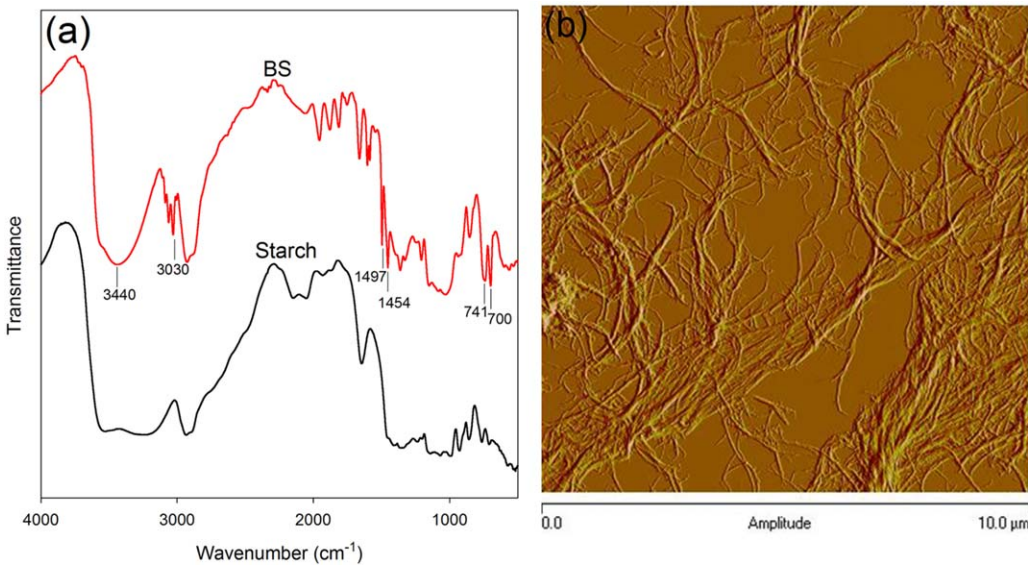

Figure 2. (a) FT-IR spectra of starch and BS, (b) AFM amplitude image of CNF deposited from aqueous suspensions. [Color figure can be viewed in the online issue, which is available at wileyonlinelibrary.com.]

length of 20 mm and a crosshead speed of 10 mm/min. Test specimens were cut from the prepared films using a bone shape press mold following the ASTM D-638 standard. Minimum five specimens of each material after conditioning at 50% relative humidity were tested. Average values of the E-modulus (calculated from the stress–strain curves), tensile strength, and elongation at break are reported.

RESULTS AND DISCUSSION

Characterization of BS and CNF

Benzylation of starch was confirmed by FT-IR analysis. In the FT-IR spectra [Figure 2(a)] of starch and benzylated starch (BS), the peak at about 3440 cm^{-1} corresponds to the presence of -OH groups. It is seen that the peak intensity corresponding to these –OH groups largely decreased in the FT-IR spectrum of BS indicating that a number of hydroxyl groups are diminished by benzylation. In addition, in the FT-IR spectrum of BS, the presence of the peaks at 700, 741, 1497, 1454, and 3030 cm^{-1} corresponding to the aromatic ring further confirmed that benzylation was occurred. Similar FT-IR characterization of BS was also reported by Cao *et al.*[9] In addition, the synthesized BS is soluble in DMF (starch was insoluble in DMF).

Figure 2(b) shows AFM amplitude image of dried CNF from diluted aqueous suspension. Cellulose is a linear polysaccharide macromolecule. During mechanical fibrillation of cellulose pulp, the fibrils and fibril aggregates are liberated by breaking of several inter-fibrillar of hydrogen bonds. AFM image [Figure 2(b)] obviously displays the existence of fibrillation with interconnected web-like nanofibers having diameters from 10 to 60 nm, as measured by using a cross-section of the height image.

Morphology of Blends and Nanocomposite

Fractured surfaces of neat PU, S-IPN blends, and S-IPN nanocomposite are presented in Figure 3. PU is the main phase in all S-IPN blends and nanocomposite. Generally, the domain size of BS dispersed in PU phase depends on the concentration of BS in PU/BS S-IPN.[9] When BS concentration is <20 wt % the fractured surfaces of PU/BS S-IPN [Figure 3(b,c)] are almost similar to that of neat PU; i.e., no phase separation was observed, whereas at higher concentration of BS (>20 wt %) a clear phase separation of PU and BS was observed [Figure 3(d), which shows the interpenetrating network of PU and BS i.e., dual phase morphology]. Therefore, it can be assumed that the PU and BS are completely miscible at lower concentration of BS (<20 wt %). Figure 3(e) shows the micrograph of fracture surfaces of PU63/BS27/CNF10 S-IPN nanocomposite in which PU to BS ratio is 70/30. Although a clear phase separation of PU and BS is seen in PU70/BS30 [Figure 3(d)], the presence of CNF created heterogeneity, and the boundary of PU and BS phases became unclear and undefined. This characteristic morphology of the S-IPN nanocomposite can be attributed to the fact that CNF are present in both PU and BS phases as well as the presence of CNF in both phases improved the phase dispersion between PU and BS through the interface interaction between PU-CNF and BS-CNF.

Gel Content and Swelling

The gel content and swelling behavior of neat PU, PU70/BS30, and PU63/BS27/CNF10 films were studied in DMF. Gel is formed when crosslinked between components of the blend exists and gel is an indicator of network structure in the blend. The gel content of the films was found to be 59, 83, and 85 wt % for neat PU, PU70/BS30, and PU63/BS27/CNF10 films, respectively. The higher gel content of PU70/BS30 compared with PU indicated that during the extraction most of BS molecules were entrapped within the PU network. Only the BS molecules which are weakly interacting with the PU were dissolved in DMF.

The swell ratio of the films was also calculated. The swell ratios were found to be 6.3, 8.5, and 4.4 for PU, PU70/BS30, and PU63/BS27/CNF10, respectively. The higher value of swell ratio of PU70/BS30 compared with the neat PU is perhaps because of

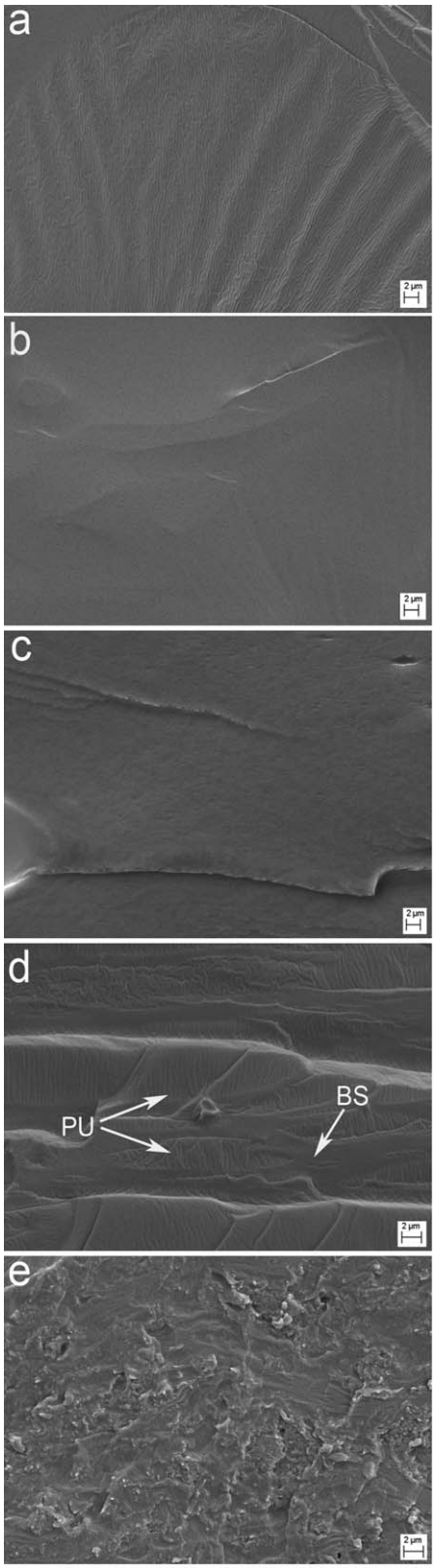

Figure 3. SEM micrographs of (a) PU, (b) PU90/BS10, (c) PU80/BS20, (d) PU70/BS30, and (e) PU63/BS27/CNF10.

the lower crosslinking density of the PU network (which can affect α-transition of PU) in S-IPN blend, whereas the lower value of swell ratio of nanocomposite can be attributed to the presence of CNF, which limit the diffusion of solvent molecules within the material.[40]

Thermo Mechanical Properties

Figure 4 displays the storage moduli (E') and tan δ values against temperature for the neat PU, S-IPN blends and nanocomposites. It is seen in Figure 4(a) that the storage modulus E' of S-IPN blends is higher compared with the neat PU, particularly, when BS concentration in the blend is >10 wt %. The values of E' of S-IPN blends in the rubbery region increased with increasing BS concentration. The E' values can also be used to calculate the filler effectiveness coefficient described as in the following equation[41]:

$$C_{FE} = \left(E'_g/E'_r\right)_{comp} / \left(E'_g/E'_r\right)_{matrix} \quad (2)$$

where E'_g is the storage moduli in the glassy region and E'_r is the storage moduli in the rubbery region of polymer and composite. The lower value of C_{FE} indicates the higher effectiveness of fillers. The values of C_{FE} reported in Table II were determined by taking E'_g and E'_r values at −40 °C and 35 °C temperature, respectively. The value of C_{FE} indicated that BS and CNF are effective fillers for PU.

Polymers miscibility can be studied by DMTA data analysis.[42] The storage modulus of neat PU decreased steadily and largely with increasing temperature. The change in the storage modulus is relatively less for S-IPN materials compared with the neat PU. The storage modulus curves of the S-IPN blends showed two separate changes in the stiffness. The first one is below 10 °C, which is related to the α-relaxation of PU and the second one is above 150 °C, which is linked with the α-relaxation of BS. However, the E' curve of PU90/BS10 steadily decreases like pure PU which indicates that a higher degree of PU and BS phase mixing in PU90/BS10 compared with the PU80/BS20 and PU70/BS30. In addition, the PU/BS S-IPN with higher BS content displayed higher storage modulus which indicates that BS increases the stiffness of the S-IPN.

The α-transition temperatures (T_α) of PU and BS are coded as $T_{\alpha 1}$ and $T_{\alpha 2}$, respectively. Remarkably, $T_{\alpha 1}$ of PU of the PU/BS films (1.9 °C for PU90/BS10) is lower than that of PU (6.8 °C) and decreased with increasing BS concentration [Figure 4(c)]. Cao *et al.*[9,43,44] also reported that many S-IPN materials based on PU and natural polymer derivatives displayed a similar trend i.e., $T_{\alpha 1}$ of PU decreases in S-IPN. This behavior can be ascribed to the fact that BS act as plasticizer to PU as well as the PU network cannot be completed because of the dilution effect of BS. Accordingly, the crosslinking density of the PU network decreases with increasing BS content. Thus, the chain mobility of the PU is enhanced.[45,46]

Although the $T_{\alpha 1}$ of PU is decreased in S-IPN blends, $T_{\alpha 1}$ of PU is increased [Figure 4(d)] markedly in nanocomposites. The positive shifting of $T_{\alpha 1}$ in S-IPN nanocomposite is an indication that CNF is dispersed in the PU. The positive shifting of $T_{\alpha 1}$ can be ascribed to the fact that the movement of PU molecules

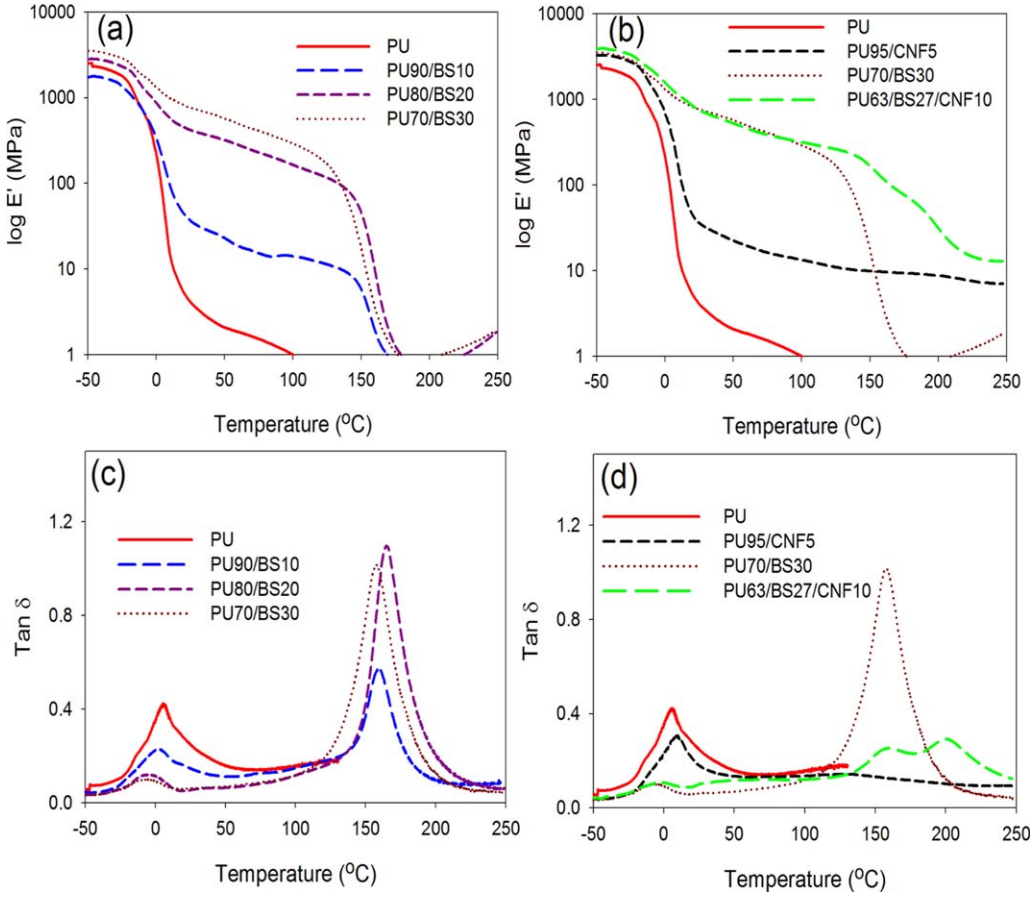

Figure 4. Effect of temperature on the storage modulus (a,b) and on the tan δ value (c,d) of PU, PU90/BS10, PU80/BS20, PU70/BS30, PU95/CNF5, and PU63/BS27/CNF10. [Color figure can be viewed in the online issue, which is available at wileyonlinelibrary.com.]

is restricted by the bond formation with hydroxyl groups of CNF. The covalent bond formation between nanocellulose and PU has also been reported by Pei *et al.* using FT-IR characterization of film.[23] Moreover, the width of tan δ peak of PU63/BS27/CNF10 nanocomposite (broadened compared with the corresponding S-IPN) also indicates higher molecular relaxations in the nanocomposite than that of neat PU and PU/BS S-IPN. It can also be noticed that the S-IPN nanocomposite displayed two T_α transitions at higher temperature, the first at about 160 °C, which can be correlated to the $T_{\alpha 2}$ transitions of BS, and the other at about 200 °C, which is probably because of some molecular interaction among BS, PU, and CNF components.

Table II. Filler Effectiveness and α-Transition Temperature of PU and its S-IPN Blends and Nanocomposites

Sample	Constant (C_{FE})	$T_{\alpha 1}$ (°C)	$T_{\alpha 2}$ (°C)
PU	1.000	6.8	—
PU90/BS10	0.077	1.9	160
PU80/BS20	0.010	−4.5	164.8
PU70/BS30	0.007	−6.3	157.8
PU63/BS27/CNF10	0.008	−1.8	159.6, 199.7
PU95/CNF5	0.146	10	—

Thermal Properties

Exemplary TA and DTA thermograms of the neat polymers (PU and BS), polymer S-IPN (PU70/BS30) and its corresponding nanocomposite S-IPN (PU63/BS27/CNF10), are shown in Figure 5(a,b), respectively. Detailed TA data up to 50 wt % of decomposition are summarized in Table III. The DTA curve (i.e., the temperature dependence of the degradation rate) of neat PU in air displayed four stages of degradation showing peaks in the region of 240–600 °C with maxima at 340 °C, 390 °C, 436 °C, and 521 °C. The first stage starting at 240 °C can be ascribed to the degradation of urethane bond,[47,48] and the stages starting at 360 °C can be ascribed to the polyol decomposition.[49] Similarly, four stages thermal degradation behavior of polyurethane prepared from palm-oil-based polyol were also reported by Henryk *et al.*[50] On the other hand, the DTA curve of PU70/BS30 and PU63/BS27/CNF10 displayed three stages of degradation showing maxima at 332 °C, 389 °C, 522 °C for PU70/BS30 and 332 °C, 392 °C, 532 °C for PU63/BS27/CNF10, respectively. Generally, polyol and isocyanate can form three types of bonds by the reaction, namely normal urethane bonds, biuret linkages, and allophanate linkages.[51] Among these three bonds, biuret and allophanate linkages are thermally less stable because their complete thermal degradation can be reached at

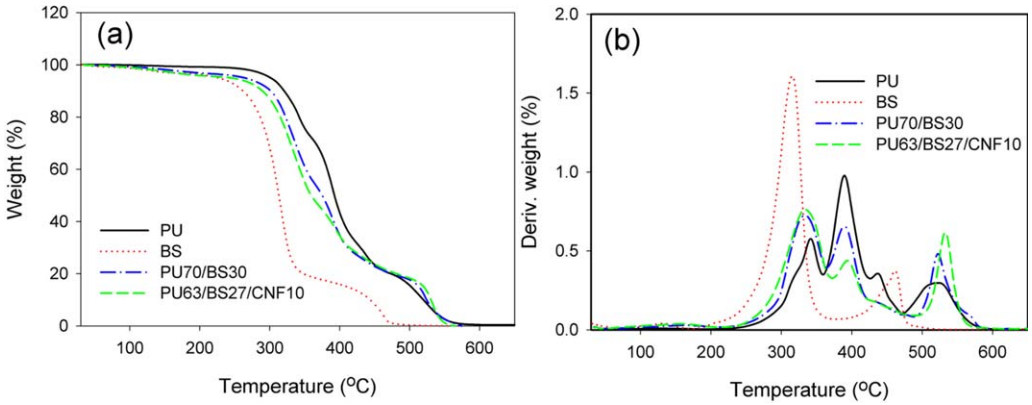

Figure 5. (a) TGA and (b) DTA graphs of PU, BS, PU70/BS30 an, PU63/BS27/CNF10 nanocomposites. [Color figure can be viewed in the online issue, which is available at wileyonlinelibrary.com.]

170–180 °C.[47,52,53] Since, below 200 °C, no weight loss was observed for the present synthesized PU, it can be concluded that there is no significant number of biuret and allophanate linkages in the present PU. Hence, the present PU exhibited more thermal resistance than others reported in the literature.[47,54] Similar high thermal resistance is also reported by Chuayjuljit *et al.*[49] after studying the thermal properties of PU synthesized from palm-oil-based polyol and PMDI. However, based on the TA traces (Table III), it can be concluded that S-IPN materials of PU/BS with and without CNF exhibited intermediate thermal resistance compared to pure components.

Mechanical Properties

Typical tensile test curves for PU and S-IPN of PU/BS with and without CNF are shown in Figure 6(a). The S-IPN materials displayed higher values of modulus and strength with respect to neat PU. In Figure 6(b), the solid bars represent strength and the patterned bars represent modulus of PU and S-IPN materials. The S-IPN, with 20 wt % BS, both the tensile modulus and strength are improved by about 2000% and 100%, respectively (modulus: from 1.7 to 35 MPa and strength: from 1.7 to 3.4 MPa) compared with the neat PU. The material with 30 wt % BS largely increased the tensile modulus and strength about 14000% and 188%, respectively (modulus: from 1.7 to 239 MPa and strength: from 1.7 to 4.9 MPa). The improved modulus of S-IPN material is because of the higher modulus of starch. However, the enhancement in tensile strength of S-IPN can be explained as under stress starch polymer chain impart to bear load with PU chain. During synthesis of S-IPN, a part of starch chain might be entrapped within the crosslinking structure of PU and the probability of entrapping can also be increased by

Table III. Temperature (°C) at Which Weight Loss Reached the Specified Levels

Sample	$T_{1\%}$	$T_{5\%}$	$T_{10\%}$	$T_{20\%}$	$T_{50\%}$
PU	241	301	321	341	391
BS	131	240	267	287	313
CNF	146	236	260	290	330
PU90/BS10	188	287	308	328	379
PU80/BS20	141	282	306	326	374
PU70/BS30	148	273	303	323	376
PU63/BS27/CNF10	137	263	293	316	360
PU95/CNF5	230	290	313	336	390

*Weight loss % data in the table were calculated considering 100% weight at 100 °C.

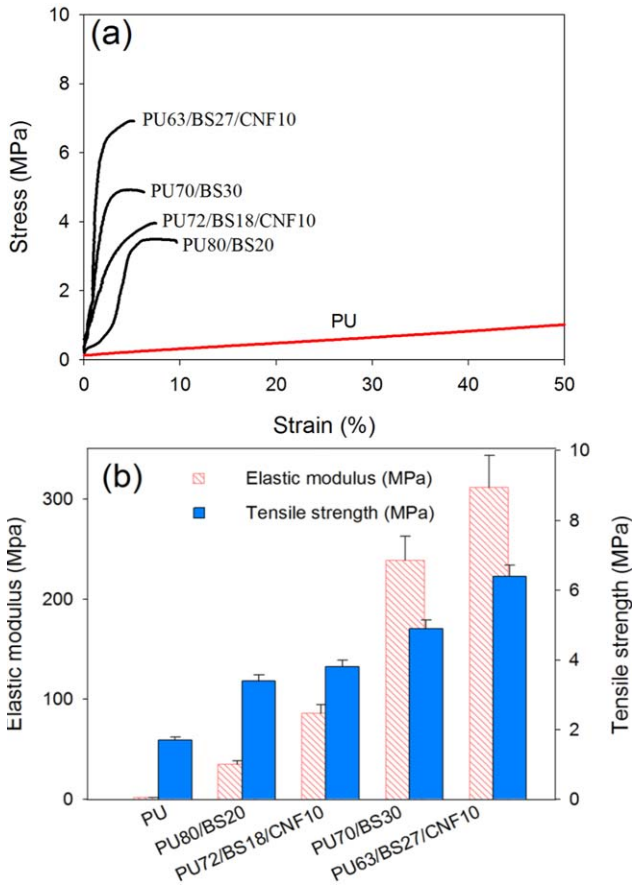

Figure 6. (a) Typical stress–strain curves, and (b) tensile modulus and strength of PU, PU/BS S-IPN blends and their nanocomposites. [Color figure can be viewed in the online issue, which is available at wileyonlinelibrary.com.]

the anchoring of benzylated part of starch chain molecule. Thus, S-IPN material can have higher tensile strength.

Further, significant improvement in tensile modulus and strength was observed in the S-IPN materials with the addition of CNF [Figure 6(b)]. The S-IPN nanocomposite with 10 wt % CNF (PU/BS ratio, 80/20) exhibited higher modulus and strength (86 and 3.8 MPa, respectively) than that of its corresponding S-IPN blend (35 and 3.4 MPa, respectively). Similarly, the nanocomposite (PU/BS ratio 70/30) also exhibited higher values of modulus and strength (312 and 6.4 MPa, respectively) than that of its corresponding S-IPN blend (239 and 4.9 MPa, respectively). This improvement in mechanical properties is expected to be because of the semi-interpenetrating network of PU and BS as well as the reinforcing effect of CNF. Although S-IPN of PU/BS with and without CNF displayed higher values of elastic modulus and strength compared with the neat PU, the elongation at break decreased compared with the soft PU which is also expected.

CONCLUSIONS

In this study S-IPN blends and nanocomposites with improved properties were prepared using renewable low cost materials such as palm-oil-based polyurethane, BS, and CNF isolated from banana rachis waste. The S-IPN films were obtained by mixing of BS (or blend of BS and CNF) with the prepolymers (polyol and isocyanate) of PU followed by casting and curing (network formation through the chemical reaction between polyol and isocyanate).

SEM study showed that PU and BS were partially miscible at lower concentration of BS. SEM study also showed that CNF are present in both PU and BS phases in the nanocomposite as well as the presence of CNF in both phases improved the phase dispersion of PU and BS.

DMTA analysis demonstrated that the α-transition peak (tan δ) of PU in S-IPN-nanocomposite was affected by both BS and CNF. The addition of BS decreased the tan δ peak position while the addition of CNF has opposite effect and it increased the position. The positive shipment of tan δ peak in nanocomposite also demonstrated that CNF were dispersed in both PU and BS phases. The data also indicated that both BS and CNF were effective reinforcement for PU.

Thermogravimetric analysis showed that S-IPN materials of PU/BS with and without CNF had intermediate thermal resistance compared with pure components.

Furthermore, the S-IPN of PU/BS with and without CNF had higher values of tensile strength and modulus compared with the neat PU. The values of tensile strength and modulus were also increased by increasing BS content in the S-IPN materials and the highest tensile strength and modulus were observed for the S-IPN nanocomposite.

ACKNOWLEDGMENTS

The authors would like to thank the Kempe Foundations and B4E strategic research program, Sweden, and TEKES in Finland for financial support. The Pontifical Bolivarian University (UPB) Colombia and PolyGreen, Malaysia are acknowledged for providing the purified/bleached cellulose pulp obtained from banana rachis waste and polyol (Polygreen 3110), respectively. We would also like to thank Natalia Herrera for AFM analysis.

REFERENCES

1. Imre, B.; Pukánszky, B. *Eur. Polym. J.* **2013**, *49*, 1215.
2. Carvalho, A.; Job, A.; Alves, N.; Curvelo, A.; Gandini, A. *Carbohydr. Polym.* **2003**, *53*, 95.
3. Chang, P. R.; Ai, F.; Chen, Y.; Dufresne, A.; Huang, J. J. *Appl. Polym. Sci.* **2009**, *111*, 619.
4. Ge, X.; Xu, Y.; Meng, Y.; Li, R. *Compos. Sci. Technol.* **2005**, *65*, 2219.
5. Santayanon, R.; Wootthikanokkhan, J. *Carbohydr. Polym.* **2003**, *51*, 17.
6. Garcia, P. S.; Grossmann, M. V. E.; Shirai, M. A.; Lazaretti, M. M.; Yamashita, F.; Muller, C. M. O.; Mali, S. *Indus. Crops. Prod.* **2014**, *52*, 305.
7. Mandal, A.; Chakrabarty, D. *Carbohydr. Polym.* **2015**, *134*, 240.
8. Cao, X.; Deng, R.; Zhang, L. *Ind. Eng. Chem. Res.* **2006**, *45*, 4193.
9. Cao, X.; Zhang, L. J. *Polym. Sci. Part B: Polym. Phys.* **2005**, *43*, 603.
10. Klempner, D.; Sperling, L. H.; Utracki, L. A. Interpenetrating Polymer Networks; No. CONF-910812; American Chemical Society: Washington, DC, **1994**,
11. Alemán, J.; Chadwick, A. V.; He, J.; Hess, M.; Horie, K.; Jones, R. G.; Kratochvíl, P.; Meisel, I.; Mita, I.; Moad, G. *Pure Appl. Chem.* **2007**, *79*, 1801.
12. Liu, C.; Ding, J.; Zhou, L.; Chen, S. *J. Appl. Polym. Sci.* **2006**, *102*, 1489.
13. Chikh, L.; Delhorbe, V.; Fichet, O. *J. Membr. Sci.* **2011**, *368*, 1.
14. Dragan, E. S. *Chem. Eng. J.* **2014**, *243*, 572.
15. Zhu, M.; Bandyopadhyay-Ghosh, S.; Khazabi, M.; Cai, H.; Correa, C.; Sain, M. *J. Appl. Polym. Sci.* **2012**, *124*, 4702.
16. Ang, K. P.; Lee, C. S.; Cheng, S. F.; Chuah, C. H. *J. Appl. Polym. Sci.* **2014**, *131*, DOI: 10.1002/app.39967.
17. Zafar, F.; Zafar, H.; Sharmin, E. *J. Appl. Polym. Sci.* **2014**, *131*,
18. Bird, S.; Clary, D.; Jajam, K.; Tippur, H.; Auad, M. *Polym. Eng. Sci.* **2013**, *53*, 716.
19. Hojabri, L.; Kong, X.; Narine, S. S. *Biomacromolecules* **2009**, *10*, 884.
20. Athawale, V. D.; Kolekar, S. L.; Raut, S. S. *J. Macromol. Sci. Part C: Polym. Rev.* **2003**, *43*, 1.
21. Vlad, S.; Vlad, A.; Oprea, S. *Eur. Polym. J.* **2002**, *38*, 829.
22. Devia, N.; Manson, J.; Sperling, L.; Conde, A. *Macromolecules* **1979**, *12*, 360.
23. Pei, A.; Malho, J.; Ruokolainen, J.; Zhou, Q.; Berglund, L. A. *Macromolecules* **2011**, *44*, 4422.
24. Marcovich, N.; Auad, M.; Bellesi, N.; Nutt, S.; Aranguren, M. *J. Mater. Res.* **2006**, *21*, 870.

25. De Rodriguez, N. L. G.; Thielemans, W; Dufresne, A. *Cellulose* **2006**, *13*, 261.
26. Beck-Candanedo, S.; Roman, M.; Gray, D. G. *Biomacromolecules* **2005**, *6*, 1048.
27. Terech, P.; Chazeau, L.; Cavaille, J. *Macromolecules* **1999**, *32*, 1872.
28. Alemdar, A.; Sain, M. *Compos. Sci. Technol.* **2008**, *68*, 557.
29. Pelissari, F. M.; do Amaral Sobral, P. J.; Menegalli, F. C. *Cellulose* **2014**, *21*, 417.
30. Abraham, E.; Deepa, B.; Pothan, L.; Jacob, M.; Thomas, S.; Cvelbar, U.; Anandjiwala, R. *Carbohydr. Polym.* **2011**, *86*, 1468.
31. Angles, M. N.; Dufresne, A. *Macromolecules* **2001**, 34.
32. Jonoobi, M.; Harun, J.; Mathew, A. P.; Oksman, K. *Compos. Sci. Technol.* **2010**, *70*, 1742.
33. Gong, G.; Pyo, J.; Mathew, A. P.; Oksman, K. *Compos. Part A: Appl. Sci. Manuf.* **2011**, *42*, 1275.
34. Hietala, M.; Mathew, A. P.; Oksman, K. *Eur. Polym. J.* **2013**, *49*, 950.
35. Pracella, M.; Haque, M. M.; Puglia, D. *Polymer* **2014**, *55*, 3720.
36. Dufresne, A.; Cavaille, J.; Helbert, W. *Polym. Compos.* **1997**, *18*, 198.
37. Herrera, N.; Mathew, A. P.; Oksman, K. *Compos. Sci. Technol.* **2015**, *106*, 149.
38. D2765-01 (reapproved 2006) Standard Test Methods for Determination of Gel Content and Swell Ratio of Crosslinked Ethylene Plastics; ASTM International, West Conshohocken, PA **2006**.
39. Barikani, M.; Hepburn, C.; Iranian, J. *Polym. Sci. Technol.* **1992**, *1*,
40. Visakh, P.; Thomas, S.; Oksman, K.; Mathew, A. P. *J. Appl. Polym. Sci.* **2012**, *124*, 1614.
41. Pothan, L. A.; Oommen, Z.; Thomas, S. *Compos. Sci. Technol.* **2003**, *63*, 283.
42. Hourston, D. J.; Schäfer, F. *Polymer* **1996**, *37*, 3521.
43. Gao, S.; Zhang, L. *Macromolecules* **2001**, *34*, 2202.
44. Lu, Y.; Zhang, L. *Polymer* **2002**, *43*, 3979.
45. Zhou, Q.; Zhang, L.; Zhang, M.; Wang, B.; Wang, S. *Polymer* **2003**, *44*, 1733.
46. Pittman, C.; Xu, X.; Wang, L.; Toghiani, H. *Polymer* **2000**, *41*, 5405.
47. Molero, C.; de Lucas, A.; Rodríguez, J. F. *Polym. Degrad. Stab.* **2008**, *93*, 353.
48. Lefebvre, J.; Bastin, B.; Le Bras, M.; Duquesne, S.; Paleja, R.; Delobel, R. *Polym. Degrad. Stab.* **2005**, *88*, 28.
49. Chuayjuljit, S.; Sangpakdee, T.; Saravari, O. *J. Metals Mater. Miner.* **2007**, *17*, 7.
50. Pawlik, H.; Prociak, A. *J. Polym. Environ.* **2012**, *20*, 438.
51. Saraf, V. P.; Glasser, W. G. *J. Appl. Polym. Sci.* **1984**, *29*, 1831.
52. Ravey, M.; Pearce, E. M. *J. Appl. Polym. Sci.* **1997**, *63*, 47.
53. Bakirova, I.; Valuev, V.; Demchenko, I.; Zenitova, L. *Polym. Sci.Series A Chem. Phys.* **2002**, *44*, 615.
54. Pielichowski, K.; Kulesza, K.; Pearce, E. M. *J. Appl. Polym. Sci.* **2003**, *88*, 2319.